DYNA
http://dyna.medellin.unal.edu.co/

UNIVERSIDAD NACIONAL DE COLOMBIA

Structural performance of composite beams using advanced modeling for nonlinear analysis

Mazin M. Sarhan [a] & Faiq M. S. Al-Zwainy [b]

[a] Department of Civil Engineering, College of Engineering, Mustansiriyah University, Iraq. mazin.m@uomustansiriyah.edu.iq
[b] Department of Civil Engineering, College of Engineering, Al-Nahrain University, Iraq. faiq.m.al-zwainy@nahrainuniv.edu.iq

Received: March 28th, 2025. Received in revised form: July 24th, 2025. Accepted: August 1th, 2025.

Abstract
A few studies used full-embedded steel sections in composite beams to reduce their cross sections. This paper presents the behavior of normal and high-strength composite beams having various heights of full-embedded steel sections. The stirrups and compression reinforcement details of the beams were the same. The finite element method was adopted in the 3D nonlinear analysis of the presented study. Full-scale composite models were investigated and tested under four-point bending. The load-deflection behavior including the elastic and post-cracking stages was monitored in this paper. Furthermore, the stress distribution of embedded steel sections, crack patterns, and modes of failure of the composite beams were investigated and studied. The results showed that the implemented analytical models were accurate, in which the error percentage was only 1.3%. The high-strength concrete composite beams showed more strength and ductile failure than those with normal strength. Also, the full-embedded steel sections have fully or partially yielded.

Keywords: concrete; composite beam; reinforcement; crack; finite elements.

Rendimiento estructural de vigas compuestas mediante modelado avanzado para análisis no lineal

Resumen
Algunos estudios utilizaron secciones de acero completamente embebidas en vigas compuestas para reducir sus secciones transversales. Este artículo presenta el comportamiento de vigas compuestas normales y de alta resistencia con varias alturas de secciones de acero completamente embebidas. Los detalles de los estribos y el refuerzo de compresión de las vigas fueron los mismos. El método de elementos finitos se adoptó en el análisis no lineal 3D del estudio presentado. Se investigaron y probaron modelos compuestos a escala real bajo flexión en cuatro puntos. En este artículo se monitoreó el comportamiento de carga-deflexión, incluyendo las etapas elásticas y post-fisuración. Además, se investigó y estudió la distribución de tensiones de las secciones de acero embebidas, los patrones de fisuración y los modos de fallo de las vigas compuestas. Los resultados mostraron que los modelos analíticos implementados fueron precisos, en los que el porcentaje de error fue de solo 1.3%. Las vigas compuestas de hormigón de alta resistencia mostraron mayor resistencia y fallo dúctil que aquellas con resistencia normal. Además, las secciones de acero completamente embebidas han cedido total o parcialmente.

Palabras clave: hormigón; viga compuesta; reforzamiento; grieta; elementos finitos.

1. Introduction

Composite reinforced concrete beams represent a pivotal advancement in structural engineering, offering enhanced strength, durability, and versatility in construction practices. This innovative approach integrates the benefits of both concrete and reinforcing materials to create robust and efficient structural elements. Key to the efficacy of composite reinforced concrete beams is their ability to distribute loads effectively, harnessing the tensile strength of reinforcing materials to complement the compressive strength of concrete. This synergy enhances structural integrity, mitigates the onset of cracks, and minimizes the propagation of failure mechanisms, thereby ensuring prolonged service

How to cite: Sarhan, M.M.S., and Al-Zwainy, F.M.S., Structural performance of composite beams using advanced modeling for nonlinear analysis DYNA, (92)238, pp. 103-110, July - September, 2025.

life and reduced maintenance costs. Moreover, composite reinforced concrete beams facilitate the realization of ambitious architectural visions, enabling the construction of slender and lightweight structural elements characterized by intricate geometries and striking aesthetics.

The performance of beams reinforced with encased sections relies on the bond strength between the section and the concrete. This bond ensures the stability and overall performance of the beam under various loading conditions. The bond allows for the effective transfer of loads between the two materials. A strong bond ensures that the forces acting on the beam are efficiently transmitted from the concrete to the reinforcing steel and vice versa [1-4]. Proper bonding also helps control cracking within the concrete, distributing the stresses effectively, and minimizing the formation and propagation of cracks [5-6]. Furthermore, adequate bond strength contributes to the long-term durability of the reinforced beam [7-8]. It helps prevent debonding, which can lead to structural failure over time due to corrosion, fatigue, or other environmental factors. Engineers may employ mechanical bonding techniques to ensure the integrity and strength of reinforced concrete structures. On the other hand, the behavior of reinforced concrete beams is experimentally monitored at only specific locations due to restrictions in the cost of testing equipment and accessories; therefore, enormous researchers have used Finite Element Modeling (FEM) in their investigations.

Finite Element Methods (FEM) plays a crucial role in analyzing the behavior of composite beams. FEM enables engineers to model complex interactions between different materials, accurately predicting the structural response of composite beams under various loads and conditions. This methodology allows for detailed analysis and optimization of composite beam designs, contributing to the development of more efficient and reliable structural systems in engineering practice. Buyukozturk (1977) [9] stands out as among the earliest researchers to pioneer a methodology aimed at incorporating the influence of reinforcements into the finite element analysis of concrete structures. Subsequently, multiple mathematical models, such as those proposed by Bergan and Holand in 1979 [10] and Vecchio in 1989 [11], were further developed to encompass the simulation of material characteristics and interactive behaviors, which serve as the origins of nonlinearities within concrete structures for Finite Element Method (FEM) analysis. Through the expansion of these methodologies, additional strategies incorporating considerations for the influences of plastic stiffness degradation were assessed in nonlinear finite element analysis, as explored by Oller et al. in 1990 [12]. Thereafter, several researchers used the simulations in beams investigation, for instance, Damian et al. (2001) [13], Wolanski (2004) [14], Hoque (2006) [15], Saifullah et al. (2011) [16], Gilbert (2012) [17], El-Mogy et al. (2013) [18], Peng and Liu (2013) [19], Tsavdaridis et al. (2013) [20], Satasivam and Bai (2014) [21].

Investigations into the behavior of structural elements demand a trustworthy finite element model. It is imperative to possess an in-depth comprehension of the appropriate elements for precise modeling, thereby guaranteeing the accuracy of response estimation. Determining an appropriate finite element model capable of accurately predicting and computing the exact responses of reinforced concrete members is highly challenging due to the complexity inherent in their behavior and nature. Various factors influence the analysis outcomes of an RC member, including yielding strain, reinforcement material's hardening effects, concrete's crack and crush behavior, material properties, section specifications, and the type of loading applied to the member. In recent years, various scholars have introduced numerous models and methodologies concerning the numerical analysis of reinforced concrete beams, for example, Hazelwood et al. (2015) [22], Qu et al. (2016) [23], and Tong et al. (2017) [24].

This study emphasizes finite element analysis modeling as a dependable and user-friendly approach for conducting nonlinear analysis on composite beams using normal-strength concrete (NSC) and high-strength concrete (HSC). The specimens were modeled and analyzed as full-scale composite beams by using ANSYS software package.

2. Research significance

The use of composite beams is a way to reduce the cross sections and increase the ultimate strength of the structure. Most previous studies used composite beams with externally connected sections, while only a few of them used encased sections due to the difficulty of implementation. Therefore, this study focused on concrete beams with fully embedded sections. In addition, according to previous studies, there is complexity and difficulty in modeling the plastic behavior of reinforced concrete using the finite element method; so, this study was intended to cover this gap as well.

3. Modeling and analysis of composite beams

The modeling process typically consumes about 40-60% of the total solution time. It holds significant importance in finite element analysis, as unexpected errors may arise during the solution phase due to improper modeling. Considerable reductions in solution time and computer memory requirements can be achieved by appropriately idealizing the structure's geometry.

Ten stages were conducted to model the investigated composite beams. The first stage involved selecting the analysis type, where structural analysis was utilized in this study. The second stage entailed selecting the element type for each material used in the beams. The third stage involved specifying the real constants of the materials, wherein the cross-section of steel bars was defined. The fourth stage entailed assigning the material properties of the element types, and defining the linearity and nonlinearity of materials. The fifth stage encompassed modeling the geometry of the beam. The sixth stage involved meshing, dividing the geometry into specific elements. The seventh stage entailed applying the loads and boundary conditions. In the current study, the loads were applied as displacement, and the boundary conditions comprised hinges and roller supports. The eighth stage involved identifying the options for nonlinear analysis. Static analysis, geometry nonlinear, displacement solution control, and the Newton-Raphson

method were employed in this step. The ninth stage was the solution. The last stage involved viewing the solution results, which included load-deflection behavior, cracks, and stresses.

4. Types of elements used in the reinforced concrete modeling

In finite element analysis, the selection of appropriate element types is a significant criterion. Table 1 displays the types of elements used in reinforced concrete modeling. The concrete was modeled using the SOLID65 element, designed especially for concrete. The treatment of nonlinear material properties is considered the most significant characteristic of this element. The SOLID65 element can be cracked in tension in three orthogonal directions, crush in compression, deform plastically, and exhibit creep behavior. The steel bars were modeled using the LINK180 element, capable of elasticity, accommodating large strains, deflections, plasticity, rotations, and creep. The steel sections were modeled using the SOLID185 element, which features stress stiffening, large strain and deflection capabilities, and plasticity.

The elements utilized in the modeling process necessitate fundamental information concerning their properties, referred to as real constants. In the case of the SOLID65 element, the real constant for the crushed stiffness factor (CSTIF) was employed either through a cracked face or for a crushed element. For the LINK180 element, the cross-sectional area of the reinforcing bars was defined as a real constant. Notably, the real constant of the SOLID185 element did not require definition.

5. Material properties

5.1 Concrete

The material properties play a significant role in structural modeling. Developing concrete behavior in finite element modeling is considered a challenging task. In this study, linear (elastic) and multi-linear (plastic) isotropic material properties were used in the SOLID65 element to model concrete behavior. The modulus of elasticity of concrete (E_c) and Poisson's ratio (v) were defined in the linear isotropic material properties. The modulus of elasticity of concrete (E_c) was calculated from eq. (1), and Poisson's ratio (v) was assumed to be equal to 0.2 for all the models.

$$E_c = 4700\sqrt{f_c'}(MPa) \tag{1}$$

Table 1.
Types of elements used in the reinforced concrete models.

No.	Modelled Material	Element Type
1	Concrete	SOLID65
2	Steel bars, stirrups	LINK180
3	Steel sections, loaded steel pieces and studs	SOLID185

Source: The authors.

In the nonlinear part, compressive uniaxial stress-strain behavior for concrete was defined. For normal-strength concrete, the stress-strain behavior was adopted based on the model proposed by Desayi and Krishnan (1964) [25], as shown in eqs. (2 and 3), along with eq. (4) proposed by Gere and Timoshenko (1997) [26].

$$f_c = \frac{E_c \varepsilon}{1 + (\frac{\varepsilon}{\varepsilon_o})^2} \tag{2}$$

$$\varepsilon_o = \frac{2f_c'}{E_c} \tag{3}$$

$$E_c = \frac{f_c}{\varepsilon} \tag{4}$$

where:

f_c = stress at any strain (ε),

ε_o = strain at the ultimate compressive strength of concrete (f'_c).

For high strength concrete, the stress-strain behavior was adopted based on the model proposed by Thorenfeldt (1987) [27], as shown below:

$$f_c = [((\varepsilon_c/x)^{y\,g} + y - 1)^{-1}]\; y\, f_c'\; (\varepsilon_c/x) \tag{5}$$

where:

$$y = (0.0588\, f_c') + 0.8 \tag{6}$$

$$x = [y/(y-1)](f_c'/E_c)] \tag{7}$$

$$E_c = 3320\; (\sqrt{f_c'} + 2.0784) \qquad (N/mm2) \tag{8}$$

$$g = \begin{cases} 1 & ,when \quad (\varepsilon_c/x) \le 1 \\ (0.0161\, f_c') + 0.67 & ,when \quad (\varepsilon_c/x) > 1 \end{cases} \tag{9}$$

The tension behavior of concrete was simulated using a linear-elastic model prior to cracking. The uniaxial tensile cracking stress was defined depending on the modulus of rupture (f_r), as shown in eq. (10).

$$f_r = 0.7\sqrt{f_c'} \tag{10}$$

5.2 Reinforcement

Steel is a homogeneous material assumed to transfer axial force only. This behavior is assumed to be identical in compression and tension. Steel reinforcement can be modeled as either a bilinear isotropic hardening plasticity material or a multilinear isotropic hardening plasticity material. The von Mises yield criterion is used in both models.

In modeling the bilinear isotropic hardening plasticity material, the modulus of elasticity of steel and Poisson's ratio were assumed to be equal to 200,000 MPa and 0.3, respectively. The strain hardening modulus (ET) was utilized to prevent convergence problems during the solution. In modeling the multilinear isotropic hardening plasticity

material, the uniaxial stress-strain behavior of steel reinforcement was defined. In the current study, compression reinforcement and stirrups were modeled using bilinear isotropic hardening plasticity materials, while tension reinforcement was modeled using multilinear isotropic hardening plasticity material.

6. Modeling and mesh generation

In the current study, the concrete and reinforcement were modeled as volumes, which were then meshed by dividing the model into finite elements. To select the best mesh, four full-scale beams (without reinforcement) were modeled in this study; the number of elements ranged between 6180 and 15720 elements. Fig. 1 shows the relationship between the failure load and the number of elements of the models.

The few elements may lead to inaccurate results, while an excessive number of elements requires significant time for the solution and a large memory area, potentially leading to convergence problems before failure. Therefore, selecting the ideal number of elements leads to reliable and accurate results. In the current study, the model with 13520 elements was selected. Details of a tested model are presented in Fig. 2.

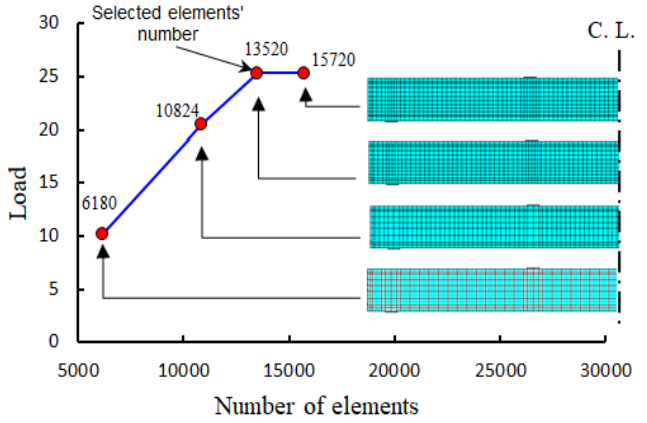

Figure 1. Mesh of concrete model.
Source: The authors.

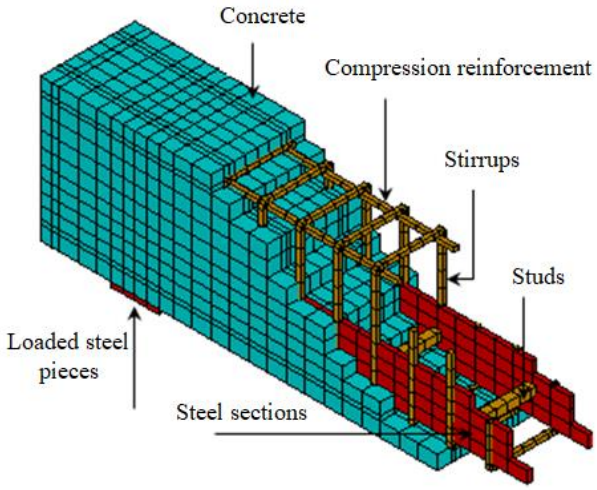

Figure 2. Models' details of a Specimen.
Source: The authors

7. Application of boundary conditions and loads

The beams' bending test of this study was performed using a 4-point bending setup in accordance of ASTM C78/C78M. Simply supports (hinge and roller) were used as boundary conditions for the models in the current study. In the hinge support, the nodes were constrained in x and y-directions. In the roller support, the nodes were constrained in y-directions. Both the supports were constrained in the z-direction to prevent the motion in the z-direction. The boundary conditions were applied across the centerline of the loaded pieces (on the bottom nodes). Fig. 3 shows the boundary conditions used in the models.

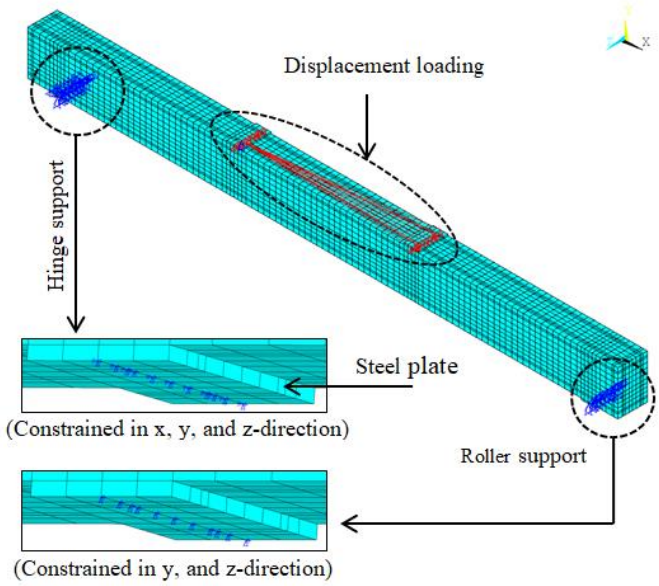

Figure 3. Boundary conditions and displacement application.
Source: The authors.

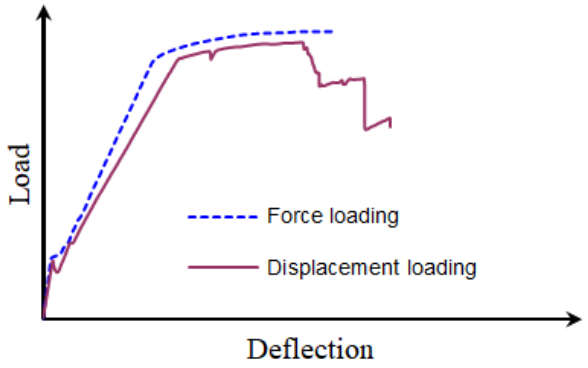

Figure 4. Methods of loads' application.
Source: The authors

Table 2.
Parametric test matrix.

Beams ID	Concrete compressive strength (MPa)	Height ofsteel sections (mm)
B1-C-35	35	100
B2-C-42	42	
B3-C-55	55	
B4-C-70	70	
B5-S-H1	42	50
B6-S-H2		75
B7-S-H3		100
B8-S-H4		131

Source: The authors.

The load can be applied by using the force or the displacement. In the case of application of the force, the force is applied on the nodes; every node takes a specific amount of the force. In the case of the application of the displacement, the couple DOFs (coupled degrees of freedom) option was used. Here, the top centreline nodes of loaded pieces were coupled in one node by using the couple DOFs option, and then a displacement was applied to this node.

Fig. 4 shows the difference between the use of force and displacement loading as was investigated in the current study. It can be clearly seen that the application of displacement is more accurate and reflect the actual behavior of models; thus, it was adopted in the investigations of this study.

8. Test matrix

Eight full-scale models were adopted to investigate the structural behavior of composite beams. The models were designed with the dimensions of 0.2 m width x 0.3 m height x 4 m length. The stirrups and compression reinforcement details of the beams were the same. The main reinforcement comprised two steel sections (with rectangular cross-sections) placed at a 90-degree angle; the thickness of the steel sections was 0.1 m, and their yield strength was 370 MPa. To enhance the cohesion between the reinforcement and concrete, the steel sections were provided with twenty steel rods equally spaced along the sections.

The test matrix was divided into two groups. The first group included four models designed with a specific concrete compressive strength for each beam, covering the normal and high-strength ranges. The second group included four models designed with a specific cross-section size of embedded reinforced sections for each beam. Table 2 illustrates the test matrix of this study.

9. Results and discussion

9.1 Behaviour of composite beams having NSC and HSC

The results include the load-deflection behavior, ultimate loads, deflection along the span, and crack patterns of the tested full-scale models. The composite beams exhibited different ultimate loads depending on the type of concrete strength (NSC or HSC). In general, and for all the beams, the ultimate loads increased with the increase in compressive

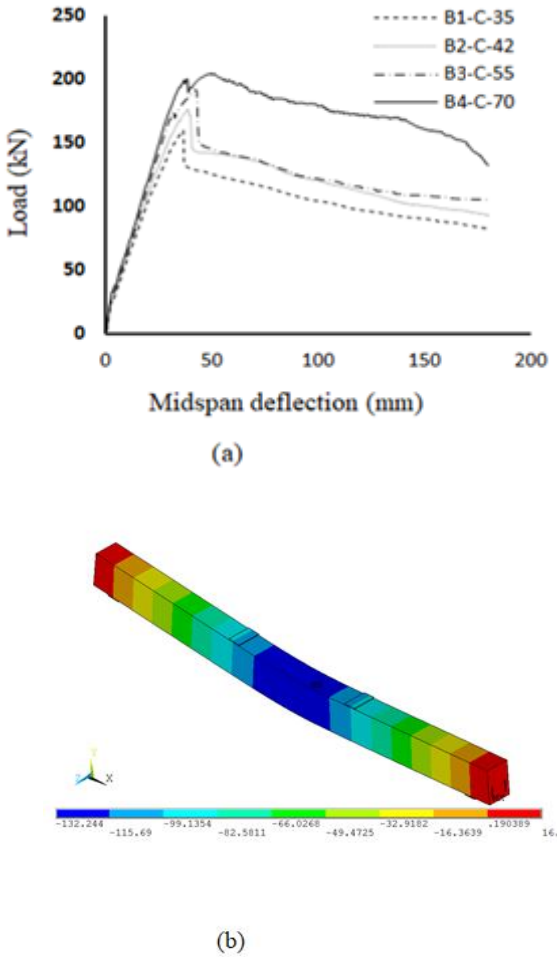

Figure 5. Behaviour of composite beams: (a) load-midspan deflection, (b) deflection along the span.
Source: The authors

strength, as shown in Fig. 5-a. The ultimate load increased by 22% when the concrete changed from NSC (35 MPa) to HSC (70 MPa). HSC exhibited lower linear elastic behavior than NSC. The concrete crush occurred before a 40 mm deflection for the beam with NSC and before a 50 mm deflection for the beam with HSC. Fig. 5-b shows the deflection along the modeled beams, with maximum deflections at the middle and minimum deflections at the ends. According to Fig. 5-a, the ductility of the tested beams enhanced when the concrete switched from NSC to HSC; however, Fig. 5-b did not present a clear enhancement trend.

During the modeling stage, it's important to consider factors such as material properties, loading conditions, boundary conditions, and structural analysis methods to predict and interpret crack patterns accurately. ANSYS program is capable of recording cracks at each loading substep. Fig. 6 shows the crack patterns of NSC and HSC beams at failure loads. Flexural cracks were caused by bending stresses in the beam and were observed along the bottom of the beam's cross-section in the vicinity of the neutral axis. Additionally, crushing cracks occurred due to high compressive forces, resulting in localized crushing or spalling of the concrete. The failure mode of all beams was flexure.

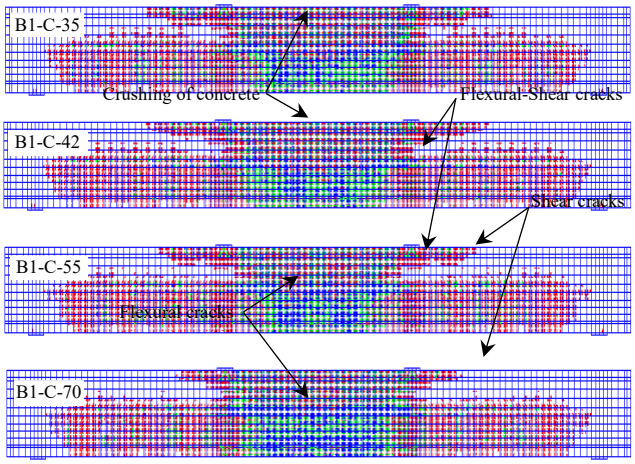

Figure 6. Cracks patterns for the modelled beams at failure.
Source: The authors

9.2 Behavior of composite beams having different heights of steel sections

Fig. 7 illustrates the midspan deflection of composite beams under load. Among the beams, Beam B5-S-H1 exhibited the lowest ultimate load compared to the others. There was only a slight difference in ultimate loads between Beams B6-S-H2, B7-S-H3, and B8-S-H4. Specifically, the ultimate load of Beam B5-S-H1 differed from that of Beam B6-S-H2 by 22%. From the analysis, it can be concluded that increasing the height of steel sections from 50 mm to 75 mm resulted in a 28% increase in the load-carrying capacity. Moreover, the load-carrying capacity was marginally improved when the height of steel sections increased by 57%.

The results also showed that the steel sections have fully or partially yielded depending on the height of the steel section. Fig. 8 depicts the state of yielding for different heights of steel sections of beams. According to Fig. 8-a, the steel sections with a height of 50 mm have fully yielded. However, the steel sections with heights of 75-131 mm have partially yielded, as shown in Fig. 8-(b-d). The maximum stresses of steel sections with heights of 50 mm, 75 mm, 100 mm, and 131 mm were 378 kN, 373 kN, 378 kN, and 385 kN, respectively. It can also be noticed that the maximum stresses were concentrated at the mid-span of steel plates for all the beams. Thus, the failure modes of all beams were flexure.

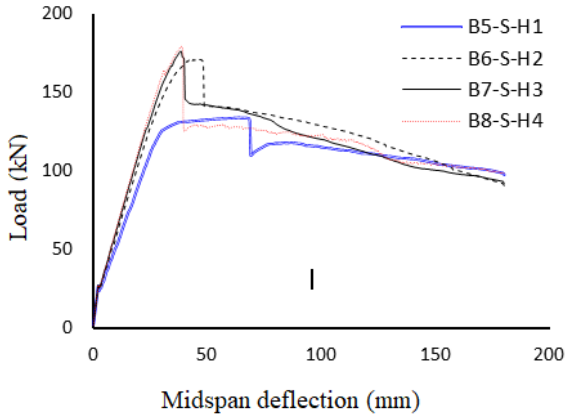

Figure 7. Load-midspan deflection curve of models of Group B.
Source: The authors

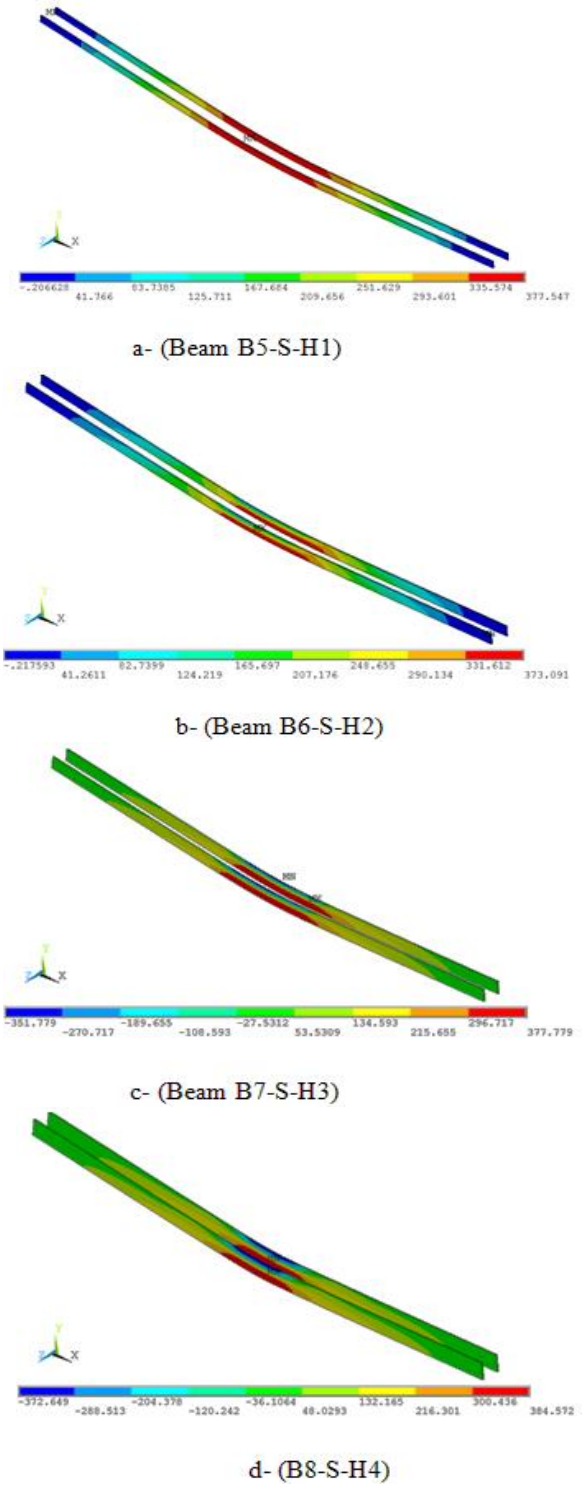

Figure 8. Stresses of steel plates with the height of: (a) 50 mm (Beam B5-S-H1); (b) 75 mm (Beam B6-S-H2); (c) 100 mm (Beam B7-S-H3); (d) 131.25 mm (Beam B8-S-H4).
Source: The authors

10. Conclusions

This research conducts nonlinear finite element analysis on NSC and HSC composite beams employing diverse steel sections. The examination of these composite beams was performed under four-point loading conditions. From the findings of this investigation, the following conclusions can be drawn:

1. There was a good agreement between the tested beams and finite element models, the difference in ultimate load was 1.3% or less. Also, the structural behavior obtained by the finite element modeling, represented by the load-deflection curves, showed good similarity with the experimentally tested beams.
2. The ductility of tested beams increased when the concrete compressive strength increased. Also, the ultimate load increased by 22% when the concrete compressive strength increased from 35 MPa to 70 MPa.
3. The steel sections have fully or partially yielded depending on the height of the steel section; the maximum stresses were concentrated at the bottom mid-span of steel sections for all the beams.
4. The use of steel sections with the heights of 50 mm to 75 mm increased the load-carrying capacity by approximately 28%, approximately. However, the use of steel sections with heights of 75 mm to 131 mm did not significantly improve the load-carrying capacity of beams.
5. The best-performimg tested beam was B4-C-70 in terms of ductility, strength and general structural behaviour.
6. The finite element models accurately predicted that the beams failed in flexure according to the appearance of cracks.

Acknowledgments

The authors would like to thank Mustansiriyah University (www.uomustansiriyah.edu.iq) Baghdad - Iraq, for its support in the present work. Also, the authors would like to thank Al-Nahrain University (www.nahrainuniv.edu.iq) Baghdad - Iraq, for its help in the current work.

Conflicts of Interest

The authors declare no conflict of interest.

References

[1] Munoz, M.B., Study of bond behaviour between FRP reinforcement and concrete, PhD. Thesis, Departament d'Enginyeria mecànica i de la construcció industrial, Universitat de Girona, Girona, Spain, 2011.

[2] Saikali, E.R., Palermo, D., and Pantazopoulou S., Bond behaviour of steel reinforcing bars embedded in ultra-high-performance steel fiber reinforced concrete, Proceedings of CSCE Annual Conference (CSCE), 2019.

[3] Basaran, B., and Kalkan, I., Investigation on variables affecting bond strength between FRP reinforcing bar and concrete by modified hinged beam tests. Composite Structures, 242, art. 112185, 2020. DOI: https://doi.org/10.1016/j.compstruct.2020.112185.

[4] Wang, X., Liu, Y., and Xin, H., Bond strength prediction of concrete-encased steel structures using hybrid machine learning method. Structures, 32, pp. 2279-2292, 2021. DOI: https://doi.org/10.1016/j.istruc.2021.04.018.

[5] Wang, L., He, T., Zhou, Y., Tang, S., Tan, J., Liu, Z. and Su, J., The influence of fiber type and length on the cracking resistance, durability and pore structure of face slab concrete. Construction and building materials, 282(2), art. 122706, 2021. DOI: https://doi.org/10.1016/j.conbuildmat.2021.122706.

[6] Niu, Y., Wei, J., and Jiao, C., Crack propagation behavior of ultra-high-performance concrete (UHPC) reinforced with hybrid steel fibers under flexural loading. Construction and Building Materials, 294(10), art. 123510, 2021. DOI: https://doi.org/10.1016/j.conbuildmat.2021.123510.

[7] Yan, F., and Lin, Z., Bond durability assessment and long-term degradation prediction for GFRP bars to fiber-reinforced concrete under saline solutions. Composite Structures, 161, pp. 393–406, art. 55, 2017. DOI: https://doi.org/10.1016/j.compstruct.2016.11.055.

[8] Lin, H., Zhao, Y., Feng, P., Ye, H., Ozbolt, J., Jiang, C. and Yang, J.-Q. State-of-the-art review on the bond properties of corroded reinforcing steel bar. Construction and Building Materials, 213(1), pp. 216–233, 2019. DOI: https://doi.org/10.1016/j.conbuildmat.2019.04.077.

[9] Buyukozturk, O., Nonlinear analysis of reinforced concrete structures. Computers and Structures, 7(1), pp. 149–156, 1977. DOI: https://doi.org/10.1016/0045-7949(77)90069-4.

[10] Bergan, P.G., and Holand, I., Nonlinear finite element analysis of concrete structures. Computer Methods in Applied Mechanics and Engineering, 2(17-18), pp. 443–467, 1979. DOI: https://doi.org/10.1016/0045-7825(79)90027-6.

[11] Vecchio, F.J., Nonlinear finite element analysis of reinforced concrete membranes. ACI Structural Journal, 86(1), pp. 26–35, 1989. DOI: https://doi.org/10.14359/2620.

[12] Oller, S., Oñate, E., Oliver, J., and Lubliner, J., Finite element nonlinear analysis of concrete structures using a "plastic-damage model". Engineering Fracture Mechanics, 35(1–3), pp. 219–231, 1990. DOI: https://doi.org/10.1016/0013-7944(90)90200-Z.

[13] Damian, K., Thomas, M., Solomon, Y., Kasidit, C., and Tanarat, P., Finite element modeling of reinforced concrete structures strengthened with FRP laminates. Report for Oregon Department of Transportation, Salem, 2001.

[14] Wolanski, A.J., Flexural behavior of reinforced and prestressed concrete beams using finite element analysis, MSc. Thesis, Department of Civil and Environmental Engineering, Marquette University, Wisconsin, USA, 2004.

[15] Hoque, M., Rattanawangcharoen, N., Shah, A.H., and Desai, Y.M., 3D nonlinear mixed finite-element analysis of RC beams and plates with and without FRP reinforcement. Computers and Concrete, 4(2), pp. 135-156, 2007. DOI: https://doi.org/10.12989/cac.2007.4.2.135.

[16] Saifullah, I., Nasir-uz-zaman, M., Uddin, S.M.K., Hossain, M.A., and Rashid, M.H., Experimental and analytical investigation of flexural behavior of reinforced concrete beam, International. Journal of Engineering and Technology, 11(1), pp. 188-196, [online]. 2011. Available at: https://shorturl.at/9MWyu.

[17] Gilbert, A.M., Validation of a laboratory method for accelerated fatigue testing of bridge deck panels with a rolling wheel load, MSc. Thesis, Department of Civil Engineering, Montana State University, Bozeman, USA, 2012.

[18] El-Mogy, M., El-Ragaby, A., and El-Salakawy, E., Experimental testing and finite element modeling on continuous concrete beams reinforced with fibre reinforced polymer bars and stirrups. Canadian Journal of Civil Engineering, 40(11), pp. 1091–1102, 2013. DOI: https://doi.org/10.1139/cjce-2012-0509.

[19] Peng, Q., and Liu, W., Inverse analysis of related parameters in calculation of concrete drying shrinkage based on ANSYS design optimization. Journal of materials in civil engineering, 25(6), pp. 683–692, 2013. DOI: https://doi.org/10.1061/(ASCE)MT.1943-5533.0000635.

[20] Tsavdaridis, K.D., Mello, C.D., and Huo, B.Y., Experimental and computational study of the vertical shear behaviour of partially encased perforated steel beams. Engineering structures, 56, pp. 805–822, 2013. DOI: https://doi.org/10.1016/j.engstruct.2013.04.025.

[21] Satasivam, S., and Bai, Y., Mechanical performance of bolted modular GFRP composite sandwich structures using standard and

blind bolts. Composite Structures, 117, pp. 59–70, 2014. DOI: https://doi.org/10.1016/j.compstruct.2014.06.011.

[22] Hazelwood, T., Jefferson, A.D., Lark, R.J., and Gardner, D.R., Numerical simulation of the long-term behaviour of a self-healing concrete beam vs standard reinforced concrete. Engineering Structures, 102, pp. 176–188, 2015. DOI: https://doi.org/10.1016/j.engstruct.2015.07.056.

[23] Qu, Y., Li, X., Kong, X., Zhang, W., and Wang, X., Numerical simulation on dynamic behavior of reinforced concrete beam with initial cracks subjected to air blast loading. Engineering Structures, 128, pp. 96–110, 2016. DOI: https://doi.org/10.1016/j.engstruct.2016.09.032.

[24] Tong, L., Liu, B. and Zhao, X.-L. Numerical study of fatigue behaviour of steel reinforced concrete (SRC) beams. Engineering Fracture Mechanics,178, pp. 477–496, 2017. DOI: https://doi.org/10.1016/j.engfracmech.2017.02.017.

[25] Desayi, P., and Krishnan, S., Equation for the stress-strain curve of concrete. International Concrete Abstracts Portal, 61(3), pp. 345-350, 1964. DOI: https://doi.org/10.14359/7785.

[26] Gere, J.M., and Timoshenko, S.P., Mechanics of Materials. ed, Boston, MA: PWS, 1997.

[27] Thorenfeldt, E., Tomaszewicz, A., Jensen, J.J., Mechanical properties of high-strength concrete and applications in design. In Proceedings of the Symposium on Utilization of High-Strength Concrete, Stavanger, Norway, 1987.

M.M. Sarhan, received the BSc. Eng in Civil Engineering from the Mustansiriyah University (Iraq) in 2006, the MSc. Eng in Civil Engineering from the Mustansiriyah University (Iraq) in 2009, and PhD from Wollongong University (Australia) in 2019. He is an inventor and got his patent in engineering field from Australia. He teaches courses for undergraduate programs in the fields of civil engineering.
ORCID: 0000-0003-2190-0342

F.M.S. Al-Zwainy, received his PhD from the Baghdad University (Iraq) in 2009. After a stint as an independent consultant in industry, when he worked on projects with local government as well as international firms, he has since held academic positions both at ISRA University (Jordan) and Al-Nahrain University (Iraq). He is an inventor and got his patent in engineering field from Australia. He teaches courses for undergraduate and postgraduate programs in the fields of applied statistics and construction project management. He is an active editor and reviewer for the KSCE Journal of Civil Engineering (Springer) and the International Journal of Engineering Sciences and Research Technology (IJESRT, open access); he is also a member of the editorial board of Civil Engineering and Urban Planning: An International Journal (AIRCC Publishing Corporation) and a member of the Project Management Institute.
ORCID: 0000-0002-9948-6594